

## Mössbauer spectroscopy of neptunyl species

G.M. Kalvius<sup>a,\*</sup>, B.D. Dunlap<sup>b</sup>, L. Asch<sup>a</sup>, F. Weigel<sup>c,✉</sup>

<sup>a</sup>Physics Department, Technical University Munich, James Franck Strasse, 85747 Garching, Germany

<sup>b</sup>Materials Science Division, Argonne National Laboratory, Argonne, IL 60439, USA

<sup>c</sup>Institute for Anorganic Chemistry, University of Munich, 8000 Munich, Germany

Received 29 April 2004; received in revised form 21 June 2004; accepted 19 July 2004

Dedicated to William T. Carnall

Available online 18 September 2004

### Abstract

Systematics of hyperfine parameters from  $^{237}\text{Np}$  Mössbauer resonance data of compounds with Np in a high formal charge state ( $\text{Np}^{6+}$ ,  $\text{Np}^{7+}$ ) are discussed with respect to electronic structure properties. In neptunyl(VI) species, we find a linear correlation between the isomer shift and the strength of quadrupole interaction. Both scale linearly with the actinide–oxygen bond length, stressing the central role of this parameter. Some compounds show paramagnetic relaxation spectra which makes their analysis difficult. The hyperfine interactions are often not rotational symmetric indicating a deviation from the simple linear O–Np–O configuration. Mössbauer spectra of  $\text{NpO}_3 \cdot 2\text{H}_2\text{O}$  reveal that this compound should be described as a neptunyl. A comparison of hyperfine parameter systematics indicates that the Np valence electron properties in Np(VII) species are basically similar to those in Np(VI) neptunyls.

© 2004 Elsevier Inc. All rights reserved.

**Keywords:** Mössbauer spectroscopy; Neptunium compounds; Neptunyl; *5f*-electron structure; Bond properties

### 1. Introduction

Recently, Mössbauer spectroscopy came into the spotlight due to the superb spectra of Martian soil returned by the Mars-landing robots. This endeavor used the workhorse of Mössbauer spectroscopy, the 14.4 keV resonance of  $^{57}\text{Fe}$  in order to determine the relative ratio of  $\text{Fe}^{2+}$  to  $\text{Fe}^{3+}$  compounds on the surface of Mars which in turn gives information on the previous presence of water. The distinction between  $\text{Fe}^{2+}$  and  $\text{Fe}^{3+}$  is possible because of the so-called isomer shift (or chemical shift). The isomer shift is unique to Mössbauer spectroscopy and has provided important chemical information not only for iron compounds but also for numerous other elements having an isotope with a suitable nuclear transition [1]. This includes in

particular the case of neptunium as a representative of light actinides. Here such information is not only of purely scientific interest, but also of importance in understanding the chemistry of compounds suitable for long-term storage, a burning issue of our time.

The isomer shift is not the only feature of a Mössbauer spectrum to give insight into chemical properties. The other hyperfine interactions (electric quadrupole and magnetic dipole couplings) are also useful for providing important information on bonding structure. Especially powerful is the combination of results for the different hyperfine parameters. In some hexavalent neptunium compounds so-called paramagnetic relaxation spectra are observed. Their analysis is in most cases complicated, if possible at all. Improper handling of such spectra can easily lead to erroneous interpretation of the spectral response, especially to misleading values for the isomer shift and thus to incorrect identification of chemical species.

\*Corresponding author. Fax: +49-89-320-6780.

E-mail address: [Michael\\_Kalvius@ph.tum.de](mailto:Michael_Kalvius@ph.tum.de) (G.M. Kalvius).

✉Deceased.

It is our aim to show that Mössbauer spectroscopy of neptunium compounds is a useful and sensitive addition to the various tools of coordination chemistry in the actinides, the field around which the scientific engagement of W. Carnall has centered. Due to the now existing severe restrictions in handling transuranic materials, most of the groups (including our own) working traditionally on Mössbauer spectroscopy in the actinides have been dissolved and the output in this field is markedly reduced. Some work still continues at laboratories especially designed for transuranic studies like the European Transuranic Institut, Karlsruhe, Germany (mainly on magnetic metallic systems) and JAERI in Japan (mainly Np chemistry).

Part of the data to be discussed here have been published previously, but are scattered in various special conference reports and not easily available to the general scientific community.

## 2. Experimental

We assume the reader to be familiar with the basic concept of Mössbauer spectroscopy. The standard procedure is to measure the transmission of the resonant  $\gamma$ -radiation through an absorber made of the compound under study as a function of the Doppler velocity of the source. The plot of relative transmission vs. Doppler velocity constitutes the Mössbauer spectrum. The special features of Mössbauer spectroscopy in actinides are explained in [2,3]. For the 60 keV Mössbauer resonance in  $^{237}\text{Np}$  one uses a source of  $^{241}\text{Am}$  metal whose emission spectrum is a single, albeit somewhat broadened line. Hyperfine interactions in Np are usually rather large and the line broadening poses no problem with respect to resolution. Using a single emission line source, the Mössbauer spectrum reflects the hyperfine interactions in the absorber and thus delivers information on the electronic properties of the sample of interest. The source is kept around liquid helium temperatures to ensure a large recoil-free fraction. The absorber may be heated up to  $\sim 100\text{ K}$ ; at higher temperatures the signal-to-noise ratio becomes poor.

## 3. Hyperfine interactions

Hyperfine interactions are the electromagnetic coupling between the nucleus (e.g.,  $^{237}\text{Np}$ ) and its surrounding electrons, primarily the electrons of its own atomic shell. Consequently, the hyperfine interactions are characterized by a nuclear and an electronic parameter. Of interest here is the electronic parameter. The nuclear parameter is either known or has to be determined in a calibration measurement. The interactions observed in Mössbauer spectroscopy are the electric monopole

coupling (isomer shift), the electric quadrupole coupling and the magnetic dipole coupling. For actinide atoms which are at the extreme end of the periodic table, relativistic effects severely complicate the theoretical treatment of the electronic parameters.

### 3.1. Isomer shift

The Coulomb interaction between the nuclear protonic charge and the charge of electrons entering the nuclear volume causes a shift of the center of gravity of the spectral pattern of a certain compound from  $v = 0$  to  $v = S$ . Strictly speaking, another contribution to the center shift, the second order Doppler effect, has to be considered. In the  $^{237}\text{Np}$  resonance this contribution is negligible and  $S$  is the isomer shift vs. the source (usual Am metal) of the compound of interest. It is given by (see [4]):

$$S = \alpha \Delta\rho_e(0) \quad (1)$$

where  $\alpha$  is the isomer shift calibration constant containing the nuclear parameter and  $\Delta\rho_e(0)$  is the difference in total electronic charge density at the nuclear origin between source and absorber material. In the relativistic limit this is due to  $s_{1/2}$  and  $p_{1/2}$  charge densities. The nuclear parameter contained in  $\alpha$  is not accessible either by other experimental techniques or by nuclear structure theories. It has to be determined by the procedure described below.

Tri-, tetra-, penta-, hexa-, and heptavalent neptunium ions are known to exist in solids. Fig. 1 shows the isomer shifts for the simple fluorides  $\text{NpF}_x$  ( $x = 3, 4, 5, 6$ ) plotted against theoretical values of  $\Delta\rho_e(0)$  for free ions having the pure  $5f^n$  ( $n = 4, 3, 2, 1, 0$ ) configurations, obtained from self-consistent Dirac–Fock calculations [5]. We then assume that the isomer shift between  $\text{NpF}_3$

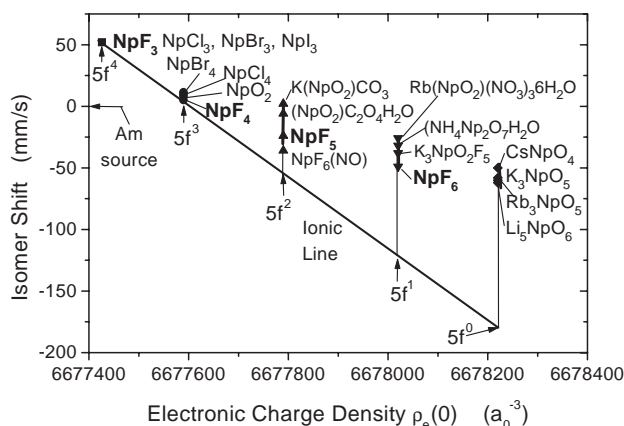


Fig. 1. Systematic of Np isomer shift. The charge density axis only refers to the ionic line through the  $5f^n$  points. The shift of the higher charged Np compounds away from this line illustrates the effect of covalency on the isomer shift. For more details see text.

and  $\text{NpF}_4$  is closest to the removal of one  $5f$  electron. Extending a straight line through these points to higher charge states produces the ‘ionic line’ whose slope gives  $\alpha \approx -0.28 \text{ mm s}^{-1}/a_0^{-3}$ . Clearly,  $f$  electrons have no charge density at the origin, but their charge distribution within the atomic shell exerts a shielding effect on the charge density at the nucleus of inner  $s_{1/2}$  and  $p_{1/2}$  electrons. A removal of a  $5f$  electrons thus leads to an increase of  $\rho_e(0)$ .

While the shifts for all trivalent halides are essentially identical, one observes already in the tetravalent halides a spread of shifts towards more positive velocities, i.e., opposite to the shift produced by the removal of a  $5f$  electron. This feature together with the strong deviation from the ionic line becomes increasingly pronounced for the higher neptunium charge states and gives evidence for the dominance of covalent bonding in these materials. Unfortunately, a quantitative interpretation of the covalency shift has met only moderate success [2] because one has to consider simultaneously  $d$ ,  $p$ , and  $s$  electron densities which have quite different influences on  $S$  not only in magnitude, but also in sign.

### 3.2. Quadrupole interaction

The electronic parameters are the electric field gradient (efg)  $eq$  and the asymmetry parameter  $\eta$  describing the deviation from rotational symmetry. The principal axes system is chosen so that  $0 \leq \eta \leq 1$ . The quadrupole interaction splits the nuclear states with spin  $I$  into sublevels characterized by the allowed numbers of  $|m_I|$ . The resonant  $\gamma$ -transitions then take place between the sublevels of the excited state and those of the ground state. For  $^{237}\text{Np}$  this leads to a symmetric (around  $\nu = S$ ) pattern of five equidistant lines if  $\eta = 0$ . For  $\eta \neq 0$  the pattern remains symmetric with the central line unaffected (which eases the extraction of  $S$ ), but the position of the other lines is no longer equidistant.

The efg consists of two components, the lattice gradient  $eq_L$ , given by the ionic charges in the crystalline lattice, and the valence gradient  $eq_V$  produced by the open shell electrons. It should be noted that for cubic point symmetry around the resonant atom one has  $eq_L = 0$ . In this case, the quadrupolar splitting vanishes altogether (due to the lack of a definite axis of quantization), meaning that  $eq_V$  cannot be obtained even if it differs from zero. In cases  $eq_L \neq 0$  the valence gradient usually dominates and the contribution by the lattice gradient can in good approximation be neglected.

### 3.3. Magnetic interaction

In a system of principal axes the magnetic interaction is given by  $\mathcal{H}_{\text{mag}} = A_x I_x J_x + A_y I_y J_y + A_z I_z J_z$  with  $J_i$  and  $I_i$  being the principal components of nuclear and electronic total angular momenta and  $A_i$  those of the

magnetic hyperfine coupling tensor. A closed form expression for the magnetic interaction energy  $E_{\text{mag}}$  is available only when a single preferred axis exist ( $A_x = A_y = 0$  and  $A_z \neq 0$ ). The problem then reduces to the well-known Zeeman interaction where a nuclear state with spin  $I$  splits into  $m_I$  equidistant sublevels separated by:  $\Delta E_{\text{mag}} = -g_I \mu_N B_{\text{hf}}$  with  $g_I = (\mu_I/I)$  being the  $g$ -factor of the nuclear state (usually known),  $\mu_N$  the nuclear magneton, and  $B_{\text{hf}}$  the hyperfine field, that is, the magnetic field at the nuclear site produced by the open shell electrons. This situation (‘effective field approximation’) prevails in long-range ordered magnets (ferro-, antiferro-, ferrimagnets) where the (sublattice) magnetization provides the quantization axis  $z$ . From the Zeeman pattern one deduces  $B_{\text{hf}}$ , which is related to the electronic structure, mainly via the total angular momentum  $J$ . The theoretical description of  $B_{\text{hf}}$  in the relativistic limit is involved [6,7] but of no particular interest here.

In a paramagnet the full tensorial interaction is usually present. The effective field approximation occurs only with uniaxial magnetic susceptibility. An additional complication arises from the spatial fluctuations of the atomic magnetic moment (or  $J$ ). If these fluctuations are rapid one encounters full motional narrowing reducing the spectrum to a single-resonance line (in the absence of an efg). If the fluctuations are slow and in particular if an efg is also present, very complex spectra with broadened and asymmetric line shapes are seen (‘paramagnetic relaxation spectra’) [8–12]. In the simplest case one has to deal with an additional spectral parameter, the fluctuation frequency  $\nu_J$ . To give the reader a glimpse of the severe effects caused by moment dynamics, we present in Fig. 2 some paramagnetic hyperfine spectra calculated for different fluctuation frequencies. Often all three hyperfine couplings are acting simultaneously in a certain compound. The isomer shift will always be present. Being isotropic, it can simply be added to any other interaction and the center shift still gives  $S$ . In case of a combined quadrupole and magnetic interaction one may have differently oriented principal axis systems for  $B_{\text{hf}}$  and  $eq$ . The three Euler angles relating to these two coordinate systems then come into play for the combined Hamiltonian.

Returning to Fig. 2, we point out, that despite the complexity of the spectral shapes shown, it represents an example with numerous simplifications. Uniaxial susceptibility is assumed. The efg is chosen to be axially symmetric and collinear to  $B_{\text{hf}}$ . The electronic ground state in the crystalline electric field (CEF) is taken as an isolated Kramers doublet, allowing replacement of the total angular momentum  $J$  by an effective spin  $S_{\text{eff}} = \frac{1}{2}$  which simplifies the dynamical calculations significantly. In the near static limit ( $\nu_J \ll 1 \text{ GHz}$ ) the pattern is determined by Lorentzian resonance lines whose

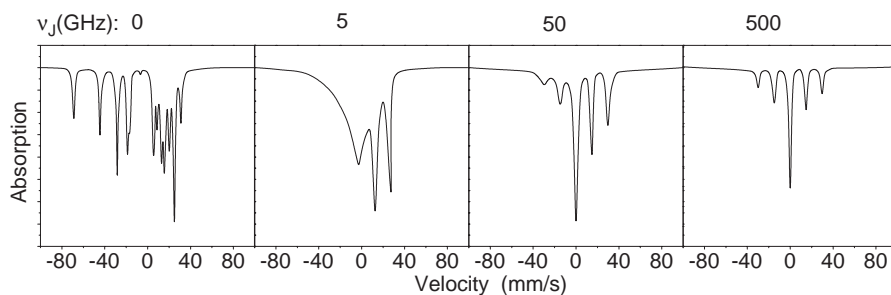


Fig. 2. Calculated paramagnetic relaxation spectra of Np for different fluctuation rates  $v_J$ . The hyperfine parameters are  $S = 0$ ,  $B_{\text{hf}} = 300$  T and a collinear quadrupole interaction  $e^2qQ = 200$  mm/s ( $Q =$  quadrupole moment of the nuclear ground state). A Kramers doublet is assumed to be the electronic ground state (see text).

positions reflect the combined Zeeman and quadrupolar interactions on the ground and excited nuclear states. Both  $B_{\text{hf}}$  and  $eq$  can be extracted with ease. The influence of electronic spin fluctuations is different for the magnetic and the quadrupole interactions [8]. In the fast fluctuation limit ( $v_J > 500$  GHz) full motional narrowing takes place for the magnetic coupling, i.e., the Zeeman splitting is wiped out. In contrast, the quadrupole splitting is not affected, meaning that a pure quadrupole pattern is seen. One can determine  $eq$ , but not  $B_{\text{hf}}$ . For intermediate fluctuation rates ( $v_J$  between 1 and 100 GHz) much of the spectral structure is lost due to the severely broadened and asymmetric line shapes. Such spectra are difficult to analyze.

#### 4. Results and discussion

A distinct feature in the chemistry of actinide compounds is the presence of the actinyl ion  $(\text{AnO}_2)^{++}$ . For neptunium it is found in hexavalent materials with the formal configuration  $5f^1$ . Generally one assumes a linear O–An–O structure. If strictly correct, a rotational symmetric efg exists. Neptunyl compounds are expected to be paramagnetic. Quadrupole and magnetic interactions occur simultaneously. For rigid O–An–O linearity the interaction will be effective. In typical cases like  $\text{Rb}(\text{NpO}_2)(\text{NO}_3)_3 \cdot 6\text{H}_2\text{O}$ ,  $\text{Na}(\text{NpO}_2)(\text{C}_2\text{H}_3\text{O}_2)_3$ , or  $(\text{NpO}_2)(\text{NO}_3)_2 \cdot x\text{H}_2\text{O}$  spectra in the static fluctuation limit are seen which can be analyzed satisfactorily in terms of a collinear rotational symmetric combined quadrupole and Zeeman interaction. The extracted values of  $B_{\text{hf}}$  vary little, centering around 300 T. We shall not pursue  $B_{\text{hf}}$  further, except to remark that this magnitude can approximately be reproduced theoretically by assuming L–S coupling and a tetragonal CEF acting on the electrons outside the actinyl core [13]. A wider variation is observed for the efg and the isomer shift (or  $\rho_e(0)$ ). Best studied by numerous other techniques are uranyl  $(\text{UO}_2)^{++}$  compounds having formally the  $5f^0$  configuration. From such data the systematics of the

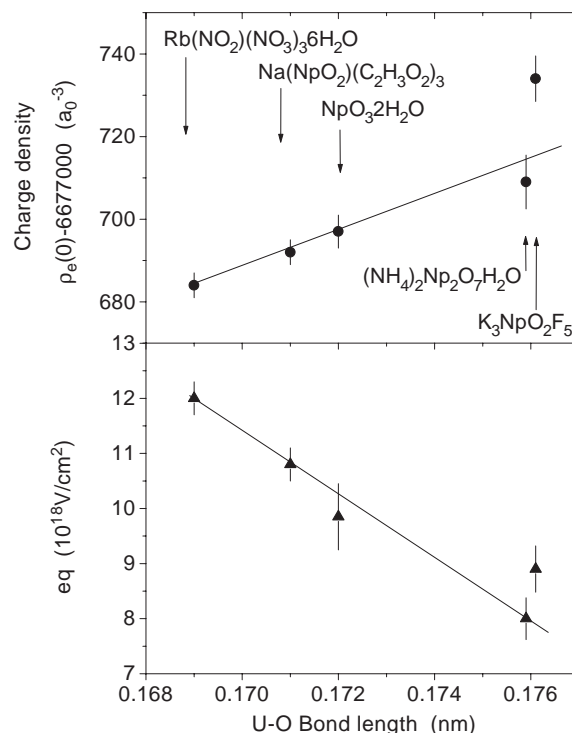


Fig. 3. Dependence of (top) charge densities at the origin ( $\rho_e(0)$ ) and (bottom) efgs of neptunyl(VI) compounds on the actinide–oxygen bond lengths in isomorphous uranyl compounds.

oxygen–uranium bond length is available with good accuracy, while Np–O bond distances are not well known. Fig. 3 shows a surprising result. Both the charge density at the origin and the efg of neptunyl(VI) species scale linearly with the U–O bond length of isomorphous uranyl compounds. Obviously, charge densities and efg are also linearly correlated. One finds  $\rho_e(0)$  to increase and  $eq$  to decrease with rising actinide–oxygen bond length. A more extended plot of the relation between isomer shift and uranyl bond length is shown in [14]. It fully confirms the relation presented in Fig. 3. The authors also put forward the notion that the full range of Np(VI) isomer shift can be grouped into several regions depending on the coordination number.



The results of Fig. 3 enlighten important aspects of neptunyl electronic structure. The most straight forward approach is to treat the  $(\text{NpO}_2)^{2+}[5f^1]$  ion as a rigid uranyl  $(\text{UO}_2)^{2+}[5f^0]$  core plus a non-bonding  $5f$  electron. The notion of rigidity for the uranyl is justified by molecular orbital calculations [15,16] which show that all available oxygen and uranium electrons are used to fill completely the existing bonding orbitals. The electronic structure is likely to be dominated by the An–O bond which is the shortest in the actinyls. Within this concept one may describe the efg of the neptunyl complex by (see Dunlap et al. [17]):

$$eq_{(\text{NpO}_2)^{2+}} = eq_{(\text{UO}_2)^{2+}} + eq_{5f}(1 - R_{5f}) \quad (2)$$

where  $eq_{5f}$  is the efg of a single non-bonding  $5f$  electron and  $R_{5f}$  is the Sternheimer factor describing the rearrangement of inner electron charge distribution by the action of the efg. Both quantities can be calculated [17] from first principles, but not the efg produced by the uranyl core. Mössbauer data obtained with the 45 keV resonance in  $^{238}\text{U}$  for uranyl compounds (e.g.  $(\text{UO}_2)(\text{NO}_3)_2 \cdot 6\text{H}_2\text{O}$ ) provide the experimental number  $eq_{(\text{UO}_2)^{2+}} = 8.2 \times 10^{-18} \text{ V/cm}^2$ . Entering this result together with the calculated value of  $eq = 3 \times 10^{-18} \text{ V/cm}^2$  for a single non-bonding  $5f$  electron outside the actinyl leads to  $eq_{(\text{NpO}_2)^{2+}} \approx 11 \times 10^{-18} \text{ V/cm}^2$  which agrees satisfactorily with the measured efg of the more strongly bound neptunyl(VI) compounds (see Fig. 3). The efg is sensitive within  $\sim 30\%$  to the actinide–oxygen bond distance, increasing with shorter bond length. A fundamental parameter determining the magnitude of an efg is the expectation value  $\langle r^{-3} \rangle$  of the electronic orbitals. The orbital radius will decrease if the molecule becomes more compact and the efg rises as observed. This supports the notion that the actinyl electronic structure is dominantly given by the An–O bond.

The situation concerning charge densities  $\rho_e(0)$  is more complex. An experimental determination of  $\rho_e(0)[(\text{UO}_2)^{2+}]$  via isomer shift measurements on uranyl compounds is not possible, because the isomer shift constant  $\alpha$  of the  $^{238}\text{U}$  resonance is practically zero (a consequence of nuclear structure [2]). The remaining approach to obtain a number for  $\Delta\rho_e(0)$  connected to the removal of one  $5f$  electron in an actinyl complex is to compare the Np isomer shifts between  $(\text{NpO}_2)^{2+}[5f^1]$  and  $(\text{NpO}_2)^+[5f^2]$ . The mean shift between corresponding penta- and hexa-valent neptunyl compounds is  $\Delta S \approx -18 \text{ mm/s}$  implying that the removal of one  $5f$  electron around the neptunyl core causes an increase of charge density  $\Delta\rho_e^{5f}(0)[\text{neptunyl}] \approx 65a_0^{-3}$ . The corresponding number for the removal of an ionic  $5f$  electron is  $\Delta\rho_e^{5f}(0)[\text{ionic}] \approx 200a_0^{-3}$  according to the ionic line of Fig. 1. This value is about three times larger because the  $5f$  electron in the neptunyl is bound in a molecular orbital, (albeit non-bonding) which has a larger radial extent than an atomic  $5f$  orbital. The increase of  $\rho_e(0)$

with bond length is in keeping with the idea that a larger orbital extent reduces the shielding effect of the  $5f$  electron on  $s_{1/2}$  and  $p_{1/2}$  charge density at the origin. Discussing solely an effect on the  $5f$  electron is perhaps an oversimplification, but one can state that  $s$  and  $p$  electrons are not dominantly influenced since this would change  $\rho_e(0)$  in the opposite direction. Only  $d$  electrons could also be involved since they generate a shielding effect similar to that of  $f$  electrons.  $\text{K}_3\text{NpO}_2\text{F}_5$  deviates somewhat from the linear relations shown in Fig. 3. It is not clear whether this is due to problems in spectral analysis or a real effect of electronic structure.

In the compounds discussed above, the  $5f$  spin relaxation is slow enough to result in a fully developed paramagnetic hyperfine pattern. Also, the spectra could be analyzed within the effective field approximation. This simple situation does not prevail in all cases. Fig. 4 shows the spectrum of  $\text{Cs}_2(\text{NpO}_2)\text{Cl}_4$  at 4.2 K which is severely distorted by paramagnetic spin fluctuations. A comparison with the shape of the simulated relaxation spectra of Fig. 2 shows that we deal with the situation of intermediate fluctuation rates  $\nu_J$  of a few GHz, but any attempt to obtain a fit under the condition of an effective interaction failed. The hyperfine interaction in  $\text{Cs}_2(\text{NpO}_2)\text{Cl}_4$  is not effective. In this case, one has to consider non-isotropic spin fluctuations, meaning that one needs to introduce three rates  $(\nu_J)_i$  with  $i = x, y, z$ , a serious additional complication. All this leads to too many degrees of freedom and the data-fitting algorithm found shallow minima in the  $\chi^2$  hyperplane for several parameter sets, none being satisfactory. A word of caution: The spectrum shown in Fig. 4 consists of a set of three fairly sharp resonance lines centered near  $v = 0$  riding on a broad spectral distribution peaking around  $v = -30 \text{ mm/s}$ . Naively, one might incorrectly interpret the spectrum as arising from two different chemical species. According to the isomer shift, these would be  $\text{Np}^{4+}$  and  $\text{Np}^{6+}$  species. Even when using the (correct) notion of the presence of a single species only, the

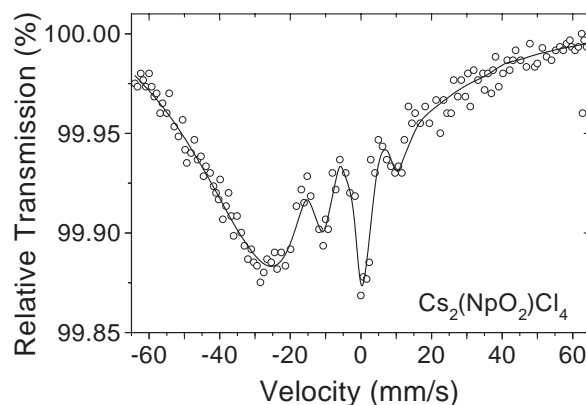


Fig. 4. Mössbauer spectroscopy of  $\text{Cs}_2(\text{NpO}_2)\text{Cl}_4$  at 4.2 K. The line is not a least-squares fit, it only serves as a guide to the eye. The spectrum should be compared with the simulation for  $\nu_J = 5 \text{ GHz}$  in Fig. 2.

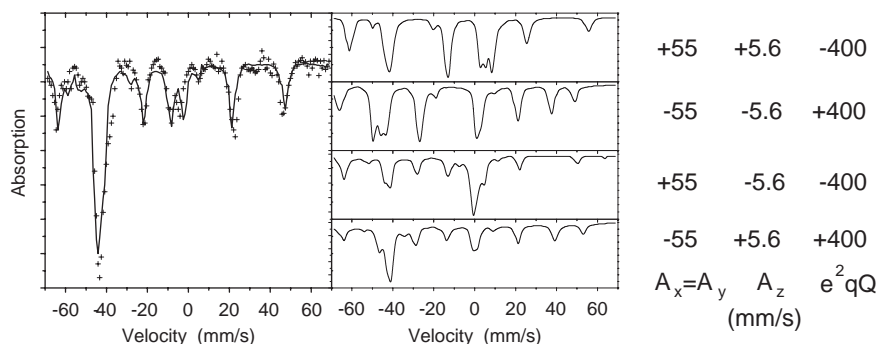


Fig. 5. Left: Measured spectrum of  $(\text{NEt}_4)_2(\text{NpO}_2)\text{Cl}_4$  at 4.2 K. The solid line is a least-squares fit based on a refinement of EPR results. Only the inner part of the spectrum is shown. Right: Simulated spectra in the static relaxation limit based on the possible choices for the hyperfine parameters given by EPR on  $(\text{NpO}_2)^{2+}$  in  $\text{Cs}_2(\text{UO}_2)\text{Cl}_4$ . Details are discussed in text.

extraction of isomer shift may be erroneous without a proper fit to the spectral response.

By replacing  $\text{Cs}^+$  with the larger cation  $[(\text{C}_2\text{H}_5)_4\text{N}]^+$  (abbreviated  $[\text{NEt}_4]^+$ ) we succeeded in reducing the spin fluctuation rate sufficiently to come close to the static limit (Fig. 5—left). Line positions immediately reveal non-effective hyperfine interaction. EPR spectra on dilute  $(\text{NpO}_2)^{2+}$  in  $\text{Cs}_2(\text{UO}_2)\text{Cl}_4$  have been analyzed under the assumption of rotational symmetry resulting in the parameter set (transformed into velocity units) [18]:  $|A_\perp| = 55 \text{ mm/s}$ ,  $|A_\parallel| = 0.1|A_\perp|$ ,  $|e^2qQ| = 400 \text{ mm/s}$ , and  $\text{sign}(e^2qQ) = -\text{sign}(A_\perp)$ . The absolute sign of the parameters could not be determined which leaves four combinations of possible signs for the hyperfine parameters shown together with the corresponding simulated spectra in Fig. 5—right. Only the combination  $A_\perp < 0$ ,  $A_\parallel > 0$  and  $e^2qQ > 0$  is roughly compatible with the measured spectrum. Starting with this set, a least-squares fit was possible, leading to  $A_x = -44.2 \text{ mm/s}$ ,  $A_y = -45.7 \text{ mm/s}$ ,  $A_z = +26.1 \text{ mm/s}$ ,  $e^2qQ = +488 \text{ mm/s}$  and  $S = -27 \text{ mm/s}$  (vs. Am metal). The value of  $S$  is in the region of highly covalent hexavalent Np compounds (see Fig. 1). Mössbauer spectroscopy detect a small deviation from rotational symmetry which EPR was not able to resolve. Also the ratio  $A_x/A_z$  is different compared to EPR, but an influence of the different cation cannot be excluded. EPR, however, could not detect any difference between  $\text{Cs}^+$  and  $\text{Rb}^+$  as cations. Finally, Mössbauer spectroscopy also allowed determination of the absolute sign of all hyperfine parameters and hence proved to be more sensitive than EPR. Warming to 77 K resulted in a pure Mössbauer quadrupole pattern, the magnetic interaction being fully motionally narrowed. This allowed an independent determination of the magnitude of  $e^2qQ$  (which agreed with the value quoted) and, more important, showed that  $\eta = 0$ . While the efg is rotational symmetric, the magnetic hyperfine coupling is not, which hints that the electronic currents in the  $(\text{NpO}_2)^{2+}$  molecule are more easily affected by a non-linearity of bond than the distribution of electronic charges.

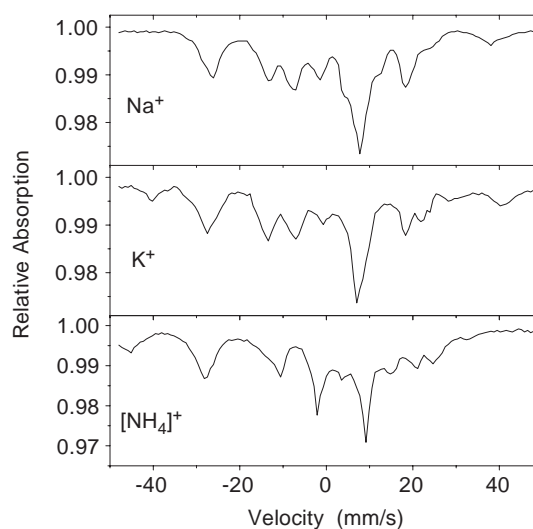


Fig. 6. Spectra of  $X_4(\text{NpO}_2)(\text{CO}_3)_3$  for different cations  $X^+$ . Since satisfactory least-squares fits were not possible (see text) the figure shows line plots of the measured spectra without treatment.

To shed more light on possible cation dependences a series of neptunyl (VI) carbonates  $X_4\text{NpO}_2(\text{CO}_3)_3$  with  $X = [\text{NH}_4]^+$ ,  $\text{K}^+$ ,  $\text{Na}^+$  was studied. Paramagnetic spectra near the static fluctuation limit were observed at 4.2 K (see Fig. 6). The interactions are not effective and once more we were not able to carry out satisfactory least-squares fits. Most likely, the efg and  $B_{\text{hf}}$  have different principal axes which leads to too large a number of ill-defined spectral parameters. The important point visible in Fig. 6 is, that line positions and intensities change with replacement of cations  $\text{Na}^+ \rightarrow \text{K}^+ \rightarrow [\text{NH}_4]^+$ . Mössbauer spectroscopy is capable of resolving distinctive variations in electronic structure on altering the cation in a series of neptunyl compounds.

Finally, we turn briefly to the Mössbauer study of  $\text{NpO}_3 \cdot 2\text{H}_2\text{O}$ . Even at 4.2 K we find a pure quadrupole pattern, the magnetic splitting being still motionally narrowed. The values of  $eq$  and  $\rho_e(0)$  fit well the systematics of the neptunyl(VI) series shown in Fig. 3

emphasizing that this material should be considered a neptunyl and be described by  $\text{NpO}_2(\text{OH})_2 \cdot \text{H}_2\text{O}$ , rather than an oxide species as often done in the literature. Noteworthy is further that the quadrupole interaction deviates significantly from rotational symmetry ( $\eta \approx 0.6$ ). It appears that the general features of electronic structure as documented by the relations shown in Fig. 3 are not affected by violating the linearity of the actinyl bond. Finally, the Mössbauer spectra of  $\text{NpO}_2(\text{OH})_2 \cdot \text{H}_2\text{O}$  demonstrate that it is difficult to prepare a pure sample of the compound. Depending on the oxidation procedure used, various amounts (typically between 10% and 40%) of a neptunium(VII) complex are present. Bulk data have to be interpreted with care. A study concerned with the preparation, crystallographic structure, and Mössbauer spectra of the hydroxide  $\text{NpO}_2(\text{OH})_2$  (i.e., without  $\text{H}_2\text{O}$ ) has recently appeared [19]. Two forms of the hydroxide ( $\alpha$  and  $\beta$ ) which are topologically similar to the corresponding well-established uranium compounds were shown to exist. For both forms pure quadrupole spectra were seen at low temperatures with parameter values roughly comparable to those of  $\text{NpO}_2(\text{OH})_2 \cdot \text{H}_2\text{O}$ . The authors agree that the Mössbauer data show that the hydroxides should be formulated as neptunyls. The observed variation in isomer shift between the  $\alpha$  and the  $\beta$  form are considered to arise by the difference in coordination number.  $\alpha$ - $\text{NpO}_2(\text{OH})_2$  exhibits a large value of  $\eta$ ; but  $\beta$ - $\text{NpO}_2(\text{OH})_2$  does not.

In all heptavalent compounds pure quadrupole spectra without any relaxation-based line broadenings were observed at temperatures between 77 K and 4.2 K. Magnetic dipolar coupling is altogether absent, proving that it arises in the hexavalent neptunyls from the single additional  $5f$  electron in its non-bonding orbital. As mentioned, this scenario has successfully been used for calculating the hyperfine field of  $(\text{NpO}_2)^{2+}$ . The ionic configuration of  $\text{Np}^{7+}$  is  $5f^0$ , but the electronic structure in heptavalent compounds is certainly not ionic. Firstly, the isomer shift deviates strongly from the ionic value (see Fig. 1). Secondly, an ionic closed shell like  $5f^0$  should not give rise to an efg. The observed values of the efg are much too large for a lattice gradient alone. The quadrupolar couplings in the  $\text{Np}^{7+}$  materials show a wide variation of asymmetry parameter ( $0 \geq \eta \geq 0.83$ ), but no correlation between the magnitude of  $eq$  and  $\eta$  could be established.

The most interesting result is that the Mössbauer spectral parameters of heptavalent neptunium compounds show the same linear relation between  $eq$  and  $S$  as previously noted in hexavalent neptunyl species (see Fig. 7). The similarity becomes especially apparent if one shifts the plot for the hexavalent neptunyls by the parameters derived previously for the removal of a non-bonding  $5f$  electron outside the actinyl core, which produces a perfect match of the two relations. This

result suggests that the valence electron structure of the Np ion in heptavalent neptunium compounds is basically the same as in neptunyl(VI) compounds minus the single  $5f$  electron in its non-bonding orbital. From this point of view, the heptavalent neptunium species are isoelectronic ( $5f^0$ ) to the uranyl  $(\text{UO}_2)^{2+}$  complex and indeed one finds that the most strongly bonded heptavalent neptunium materials exhibit a quadrupole interaction of about the same size as observed in uranyl compounds ( $\sim 8 \times 10^{18} \text{ V/cm}^2$ ).

Extrapolating the linear relation of Fig. 7 to  $eq = 0$  gives an isomer shift of  $S \approx 60 \text{ mm/s}$  which, according to an extrapolation of the shifts between  $\text{NpF}_5$  and  $\text{NpF}_6$  in the systematics shown in Fig. 1, corresponds to the isomer shift value expected for  $\text{NpF}_7$  if it were to exist. This number is still far away from the expected  $5f^0$  point, making clear that ionic bonding does not exist in compounds containing highly charged neptunium.

On occasion we have stated that the relation shown in Fig. 7 indicate a neptunyl like bond structure in the heptavalent neptunium species. This is too general a statement which has to be understood in its proper context. Contemporary research combining theoretical calculations and experimental data for solid state structures and solution coordination environments [20,21] has shown that  $\text{Np}^{7+}$  species do not possess the neptunyl(VI) linear dioxo unit, but rather a distorted tetraoxo unit with two additional long axial ligands. As outlined earlier, the hyperfine parameters of the neptunium Mössbauer spectra are nearly exclusively determined by the electrons close to the central neptunium nucleus and among those the radial factor  $\langle r^{-3} \rangle$  gives most weight to the valence electron orbitals with the smallest radial extend. These are the O–Np–O bonds, while the HO–Np–OH bond has a considerably

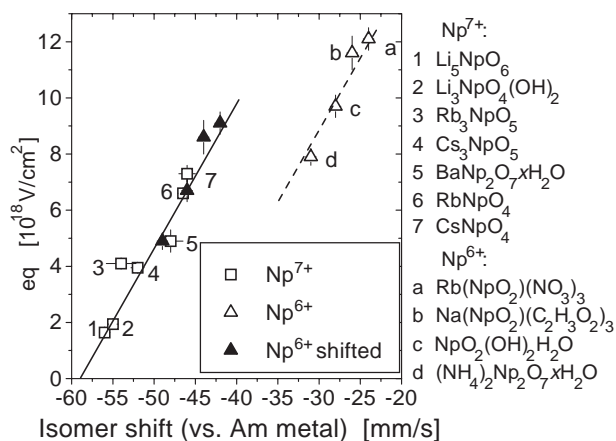


Fig. 7. Linear correlation between the efg and the isomer shift of  $\text{Np}^{7+}$  compounds. The corresponding relation for neptunyl(VI) species is shown on top right. Shifting the  $\text{Np}^{6+}$  plot by the values of  $eq = -3 \times 10^{18} \text{ V/cm}^2$  and  $S = -18 \text{ mm/s}$  corresponding to the removal of a single non-bonding  $5f$  electron leads to a perfect match of the correlations in the two series of Np materials.

larger bond length (see, for example, the structural drawings in Ref. [21]). The combined results of Figs. 7 and 3 then reveal that the local electron structure of the neptunium ion behaves alike in uranyl, neptunyl(VI) and  $\text{Np}^{7+}$  materials with the actinide–oxygen bond length being the decisive parameter. In simple words, the neptunium nucleus sees basically the same electron structure in the three types of compounds. The additional non-bonding  $5f$  electron in the neptunyl(VI) species has little, if any, influence on the behavior of  $eq$  or  $S$ . It is responsible for the paramagnetism of neptunyls(VI). Bolvin et al. [21] state that no major rearrangements on electron transfer are necessary between  $\text{Np(VI)}$  and  $\text{Np(VII)}$ . Our Mössbauer results agree perfectly with this notion.

Bond properties like overall bond symmetry and the addition of a hydroxy bond cause only small variations in the Mössbauer spectral parameters at best. For example, they might be the source of the variation in asymmetry parameter  $\eta$ . As said, the quadrupole interaction in  $\text{Np}^{7+}$  compounds reflects the behavior of the valence efg, meaning that the presence of an asymmetry parameter  $\eta$  must be caused by a distortion of the ideal square planar  $\text{Np-O}$  bond at least in solid materials. This corresponds to the violation of the pure linear dioxy bond in neptunyl(VI) species discussed earlier. The origin are possibly the more distant ligands. For example,  $\text{Li}_5\text{NpO}_6$  was expected to have octahedral symmetry which is, however, incompatible with the value of  $\eta = 0.31$  observed in its Mössbauer spectrum. It is likely that ligand bonding compresses the octahedron along one axis together with a rhombical distortion in the  $xy$ -plane [22]. The influence of distant ligands might also be responsible for the scatter of  $S$  and  $eq$  around their linear correlation lines. This has not been pursued. It would require spectral data of high precision and also that one is certain to have used the correct hyperfine Hamiltonian in the data analysis.

## 5. Conclusions

$^{237}\text{Np}$  Mössbauer spectroscopy shows that covalency characterizes the chemical bond in highly charged Np species, including the simple fluorides. The hyperfine parameters derived from Mössbauer spectra of neptunyl(VI) compounds are consistent with the model of a rigid uranyl core plus a  $5f$  electron in a non-bonding orbital. Their dependence on actinide–oxygen bond length indicate that the main effect on altering the size of the actinyl complex is the corresponding change in radial extent of the molecular orbitals rather than a basic rearrangement of electronic structure. In some compounds deviation from rotational symmetry of the hyperfine interaction was observed demonstrating that in these cases the  $\text{O-An-O}$  bond is no longer linear. This

effect appears, however, to have no significant effect on the properties of the electrons in the actinyl core stressing the importance of bond length. It may be caused by the bond to the cation, and thus not affect the actinyl core by much. Care has to be exercised in cases, where the Mössbauer spectra show strong effects of paramagnetic moment fluctuations. A reliable extraction of electronic parameters is difficult at best and even then not always possible. Misinterpretations are quite possible. A comparison with related EPR data shows that Mössbauer spectroscopy gives finer details on electronic structure. In particular, it could be demonstrated that changing the cation in a given neptunyl series results in weak, but noticeable alterations of electronic parameters. The systematics of hyperfine parameters in heptavalent Np compounds exhibits similar features to those seen in the hexavalent compounds, indicating that the properties of the neptunium valence electron structure are not fundamentally different in the two cases. From this point of view the neptunyl(VII) bond is isoelectronic to the uranyl bond, a notion which is supported by the size of the efgs found in those two species. Strong deviations from rotational symmetry of the electron charge distribution at the nucleus are seen in the heptavalent compounds meaning a violation of the ideal square planar bond geometry probably caused by the influence of more distant ligands.

## Acknowledgments

Work performed at Munich was supported by the Federal Minister for Research and Technology (BMFT), Germany. Work performed at the Argonne National Laboratory was supported by the US Department of Energy (DOE), BES-Materials Science, Contract No. W-31-109-Eng-38.

## References

- [1] G.K. Shenoy, F.E. Wagner (Eds.), Mössbauer Isomer Shifts, North-Holland, Amsterdam, 1978.
- [2] B.D. Dunlap, G.M. Kalvius, in: A.J. Freeman, G.H. Lander (Eds.), Handbook on the Physics and Chemistry of the Actinides, vol. 2, North-Holland, Amsterdam, 1985, p. 329 ff.
- [3] W. Potzel, G.M. Kalvius, J. Gal, in: K.A. Gschneidner, L.R. Eyring, G.H. Lander, G.R. Choppin (Eds.), Handbook on the Physics and Chemistry of the Rare Earths, vol. 17, North-Holland, Amsterdam, 1993, p. 539ff.
- [4] B.D. Dunlap, G.M. Kalvius, in: G.K. Shenoy, F.E. Wagner (Eds.), Mössbauer Isomer Shifts, North-Holland, Amsterdam, 1978, p. 17ff.
- [5] J.P. Desclaux, A.J. Freeman, J. Magn. Magn. Mater. 18 (1978) 119.
- [6] B.D. Dunlap, in: I. Gruverman (Ed.), Mössbauer Effect Methodology, vol. 7, Plenum Press, New York, 1972, p. 123ff.



- [7] B.D. Dunlap, G.M. Kalvius, in: A.J. Freeman, J.B. Darby (Eds.), *The Actinides: Electronic Structure and Related Properties*, Academic Press, New York, 1978, p. 237ff.
- [8] M. Blume, J. Tjon, *Phys. Rev.* 165 (1968) 446.
- [9] H.H. Wickman, G.K. Wertheim, in: V.I. Goldanskii, R.H. Herber (Eds.), *Chemical Applications of Mössbauer Spectroscopy*, Academic Press, New York, 1968, p. 428ff.
- [10] L.L. Hirst, *J. Phys. Chem. Solids* 31 (1970) 655.
- [11] G.K. Shenoy, B.D. Dunlap, *Phys. Rev. B* 13 (1976) 1353.
- [12] S. Dattagupta, G.K. Shenoy, B.D. Dunlap, L. Asch, *Phys. Rev. B* 16 (1977) 3893.
- [13] B.D. Dunlap, G.M. Kalvius, *J. de Phys. Colloids* 40 (1979) C6–C55.
- [14] J. Jové, L. He, J. Proust, M. Pages, P. Pykkö, *J. Alloy Compounds* 177 (1991) 285.
- [15] S.P. McGlynn, J.K. Smith, *J. Mol. Spectrosc.* 6 (1961) 164, 188.
- [16] C.Y. Yang, K.H. Johnson, J.A. Horsley, *J. Chem. Phys.* 68 (1978) 1001.
- [17] B.D. Dunlap, G.M. Kalvius, G.K. Shenoy, *Phys. Rev. Lett.* 26 (1971) 1085.
- [18] L.A. Boatner, M.M. Abraham, *Rep. Progr. Phys.* 41 (1978) 87.
- [19] M. Nakata, T. Kitazawa, T. Saito, J. Wang, M. Takeda, T. Yamashita, M. Saeki, *Bull. Chem. Soc. Japan* 76 (2003) 1375.
- [20] C.W. Williams, J.P. Blandeau, J.C. Sullivan, M.R. Antonio, B. Bursten, L. Soderholm, *J. Am. Chem. Soc.* 123 (2001) 4346.
- [21] H. Bolvin, U. Wahlgren, H. Moll, T. Reich, G. Geipel, T. Fanghänel, I. Grente, *J. Phys. Chem. A* 105 (2001) 11441.
- [22] K. Fröhlich, P. Gütlich, C. Keller, *J. Chem. Soc. Dalton Trans.* 971 (1972).